Pergamon

Engineering Fracture Mechanics Vol. 57, No. 2/3, pp. 319–332, 1997
Published by Elsevier Science Ltd
Printed in Great Britain
0013-7944/97 $17.00 + 0.00

PII: S0013-7944(97)00010-6

FRACTURE SIMULATIONS OF CONCRETE USING LATTICE MODELS: COMPUTATIONAL ASPECTS

E. SCHLANGEN
Intron SME, P.O. Box 226, NL 3990 GA Houten, The Netherlands

E. J. GARBOCZI
National Institute of Standards and Technology, Building Materials Division, 226/B350, Gaithersburg, Maryland, U.S.A.

Abstract—This paper addresses some lattice model techniques used in numerical simulations of fracture in concrete and other random materials. The influence of lattice element type and lattice orientation on the fracture pattern was investigated by simulating a shear loading experiment on a concrete plate. Beam elements with three degrees of freedom per node, and with a random orientation of the beams within the lattice, gave the best comparison with experiment. The effect of element resolution on fracture results was also investigated. A new fracture law has been developed that uses principal tensile stresses in each node of the lattice to determine which beam should break at every step of a simulation. For the implementation of heterogeneity in the model, a method has been developed that uses digital images of the real microstructure of a material. Simulated crack patterns were obtained for a real material, using this technique, which appear quite realistic. Published by Elsevier Science Ltd.

1. INTRODUCTION

RANDOM HETEROGENEOUS materials have complicated fracture mechanisms, which are related to their microstructure. The use of linear elastic fracture mechanics to analytically describe these mechanisms is arduous, since the fracture patterns consist of a main crack, with various branches, secondary cracks and microcracks. Numerical tools are a good option to gain some insight into the problem. Studies in theoretical physics have indicated that lattice type models can be quite successful for the simulation of fracture processes in heterogeneous materials [1]. These models have been adopted for specific applications like simulating fracture in concrete [2, 3] or in ceramics [4, 5]. Related papers using similar techniques to study the random fracture problem include refs [6–21].

In these models a material is discretized as a lattice or mesh consisting of small spring or beam elements that can transfer forces, as shown in Fig. 1. Fracture is simulated by performing a linear elastic analysis of the lattice under loading and removing (or partially removing) an element from the mesh that exceeds a certain threshold for quantities such as strength or energy. Differences in strength and stiffness between different regions in a random material can be incorporated by adjusting the tensile strength and the modulus of beams that fall in these regions.

An example of a random material with these kind of differences is concrete. Concrete consists of sand and rock inclusions (aggregates) embedded in a cement paste matrix. The sand size typically ranges up to a few mm in diameter, while rock size ranges up to 30 or 40 mm. A concrete prepared with only sand aggregates is called a mortar. There is a weak interface found in concrete between the aggregates and the cement paste matrix that can dominate the properties of the material [22]. This interface can be handled in a fracture simulation by adjusting the tensile strength and the modulus of beams that fall in this region, as well as allowing for differences between aggregates and cement paste matrix [3].

The results obtained from simulations with lattice models, however, can depend strongly on the fracture criterion used and the chosen element and/or mesh type. Also, it is important that the way disorder is implemented in the model, and the actual heterogeneity of the material simulated, be as close as possible.

In this paper the elastic equations as well as the fracture procedure of the model are explained in detail. Different solution techniques for the set of linear equations generated by the meshes and elements used are discussed. In Section 3, the differences in crack patterns obtained

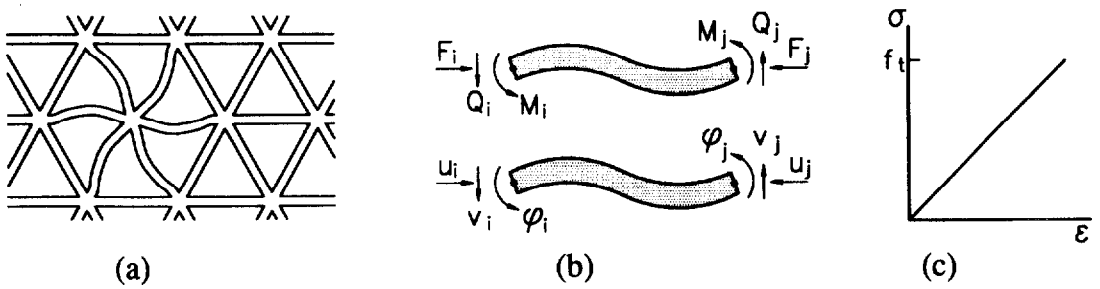

Fig. 1. (a) Regular triangular lattice of beams, (b) external forces and deformations on a single beam element, and (c) stress–strain relation for an element. (Reprinted from ref.[32].)

from simulations where the element type, beam length and mesh orientation are varied, will be shown. Furthermore the effect of various fracture criteria on the simulated crack patterns is presented. A short discussion is also given of various methods of implementing disorder in the lattice and how to relate this disorder to the actual microstructure of the material. Much of the material in this paper can also be found in ref.[23].

2. ELASTIC EQUATIONS OF LATTICE MODEL

2.1. *Set of equations*

In this section the elastic equations of the two-dimensional lattice model with beam elements will be described. Each of the beams in the lattice can transfer, in general, normal force (F), shear force (Q) and bending moment (M) as shown in Fig. 1(b). The relations among these forces and the corresponding displacements [Fig. 1(b)] for the endpoints (i and j) of a beam can be expressed as follows:

$$F_i = \frac{EA}{l}(u_i - u_j) \tag{1}$$

$$Q_i = \frac{12EI}{l^3}(v_i - v_j) - \frac{6EI}{l^2}(\phi_i - \phi_j) \tag{2}$$

$$M_i = \frac{6EI}{l^2}(v_j - v_i) + \frac{4EI}{l}\left(\phi_i - \frac{\phi_j}{2}\right) \tag{3}$$

in which E is Young's modulus, l is the length, A is the cross-sectional area and I is the moment of inertia of a beam element, (u,v) are the translational displacements and ϕ is the nodal rotation. Equations (1)–(3) use simple beam theory[1]. For a lattice with a regular geometry, like that shown in Fig. 1(a), the quantities E, l, A and I are, in principle, equal for all elements. However, these parameters can be varied, either element by element or according to a superimposed microstructure, in order to implement heterogeneity.

To construct the system of equations for the complete lattice, each element matrix has to be multiplied by the appropriate rotation matrix [24] and positioned correctly in the system matrix. The final set of equations for the system is of the form:

$$\mathbf{b} = \mathbf{A}\mathbf{x}, \tag{4}$$

in which $\mathbf{b}$ is the force (load) vector, $\mathbf{A}$ is the stiffness matrix and $\mathbf{x}$ is the displacement vector. If there are N nodes in the system, then $\mathbf{b}$ and $\mathbf{x}$ are of length $3N$, and $\mathbf{A}$ is in general a $3N \times 3N$ matrix. $\mathbf{A}$ is very sparse, however, so only a few elements per node need be stored.

2.2. *Solving the equations*

When solving the set of linear elastic equations for a lattice under an applied load, the load vector and stiffness matrix are known and the displacement vector is to be determined by solving eq. (4). One method to solve the set of equations is to use a direct solver which finds the inverse of A by Gaussian elimination[25]. A faster way to find a solution for the set of equations

is by the conjugate gradient method [26]. Recently [24], a special version of a conjugate gradient solver was implemented in the lattice model [27]. In this algorithm the displacement vector $\mathbf{x}$ is solved iteratively by minimizing the functional G, which has the dimensions of energy,

$$G = 0.5\mathbf{x}\mathbf{A}\mathbf{x} - \mathbf{b}\mathbf{x}. \tag{5}$$

The advantage of a conjugate gradient solver becomes even greater for fracture simulations. Breaking an element and thus removing it from the lattice is a local effect. This implies that the resulting changes in the deformation vector and in G will be localized near the removed element, and small elsewhere. Therefore, only a few iterations will be needed to relax the system again to find the next element to remove. It should be noted that more iterations of the algorithm are necessary to converge to a solution when property differences between components of the system become large. This will happen, for example, when simulating a multi-phase composite where one phase is much stiffer than the other phases. In that case, preconditioning of the $\mathbf{A}$ matrix can help to speed up the process [28].

When a direct solver is used, the complete system usually has to be re-solved every time an element is removed. However, in this case the method of structural variation could also be used [29, 30]. In this method, the inverse of the matrix $\mathbf{A}$ is used to update the displacement vector when an element is removed from the mesh, so that a full-scale solution is not needed every time. This does require a large amount of computer memory, since the inverse matrix must be stored. Although the stiffness matrix for a lattice of beams is sparse, the inverse of that matrix is generally not sparse. For a general system of N nodes, the inverse of $\mathbf{A}$ is of size $(3N)^2$, which can be enormous for typical system sizes. Clearly, the method of structural variation will be useful only for small systems.

2.3. *Elastic moduli and fracture criterion*

The 2-D elastic moduli tensor for a regular triangular lattice of beams, which is elastically isotropic, can easily be derived analytically by evaluating the elastic energy of a unit cell of the lattice under a uniform strain (hydrostatic or simple shear) [31]:

$$\text{bulk modulus}: \ \kappa = \frac{\sqrt{3}}{2}\frac{EA}{l} \tag{6}$$

$$\text{shear modulus}: \ \mu = \frac{\sqrt{3}}{4}\frac{EA}{l}\left(1 + \frac{12I}{Al^2}\right) \tag{7}$$

$$\text{Poisson's ratio}: \ \nu = \frac{\kappa - \mu}{\kappa + \mu} = \frac{\left(1 - \dfrac{12I}{Al^2}\right)}{\left(3 + \dfrac{12I}{Al^2}\right)} \quad -1 < \nu < \frac{1}{3}. \tag{8}$$

For rectangular beam elements with unit thickness and width h the Poisson ratio is equal to:

$$\nu = \frac{\left(1 - \left(\dfrac{h}{l}\right)^2\right)}{\left(3 + \left(\dfrac{h}{l}\right)^2\right)}. \tag{9}$$

To simulate fracture a breaking rule must be defined. Different criteria for fracture have been adopted and can be found in the literature [1, 5, 32–34]. The main idea is that an element of the lattice will break when a predefined threshold for some quantity, for example tensile stress or elastic energy, is exceeded in that element. Instead of removing just one element, more elements can be removed from the lattice before relaxing the system again, resulting in a method to simulate dynamic instead of just static loading. However, a relation would still have to be determined between the actual loading rate and the number of elements removed in a single time step.

In the simulations to be described in Section 3, a beam is removed from the lattice during each step whenever the following condition holds:

$$\frac{F}{A} > f_t, \tag{10}$$

where F is the normal tensile force in the beam, A is the cross-sectional area and f_t is the tensile strength of the beam. Thus, the local behaviour of a beam element is perfectly brittle. The stress–strain relation of such an element is plotted in Fig. 1(c). After removing one beam element the system is relaxed again. An error can be made when using this fracture law in a uniform lattice, which will be discussed in Section 4.

3. ELEMENT AND MESH DEPENDENCY

3.1. *Influence of element type on the crack pattern*

A lattice of springs or beams is a discretization of a continuum. The number of forces that can be transmitted by the elements of a lattice determines the type of continuum that is represented by the lattice. In this section a comparison is made between results of fracture simulations using regular triangular networks with different kinds of elements. The experimental results shown in Fig. 2(a) were simulated with elements that can transmit 1, 2 or 3 kinds of forces, respectively. In the experiment [35], a concrete plate was loaded in shear. The crack pattern that was found in the test is plotted in Fig. 2(a).

In the first simulation [Fig. 2(b)] the elements can only transfer normal force, and thus the lattice is equivalent to a central force spring network [2, 36, 37]. Equation (1) corresponds to this network. This network is a discretization of a linear elastic continuum with a value of the Poisson ratio fixed at 1/3. In the second simulation [Fig. 2(c)], the elements can also support a shear force, incorporating eq. (1) and half of eq. (2), i.e. $Q_i = 12EI/l^3(v_i - v_j)$. These elements with normal force and shear force are isomorphic to a spring network with central force plus rotational springs [4, 5]. This second network is a discretization of a linear elastic continuum with a general value of Poisson's ratio (but less than 1/3). In the third case [Fig. 2(d)] elements with normal force, shear force and bending moments are used [3, 5, 38]. Here all three equations, eqs (1)–(3), must be included. This lattice is a discretization of a higher order continuum, a Cosserat elastic continuum [1], again with a general value of Poisson's ratio less than 1/3. For a more complete overview of different lattice models the reader is referred to ref. [1].

The results of the three simulations are shown in Fig. 2(b)–(d). In the simulations no heterogeneity was implemented, so as to draw a distinction between the separate problems of disorder implementation and the ability of a lattice to describe a continuum. The crack patterns differ appreciably between the lattices with different elements. In the lattice with only normal force in the elements, one straight crack is obtained. When two degrees of freedom per node are used, the cracks start at the correct angle, but the cracks stay straight and do not curve. In the simulations with the beams able to transmit three kinds of forces, the crack pattern is much clo-

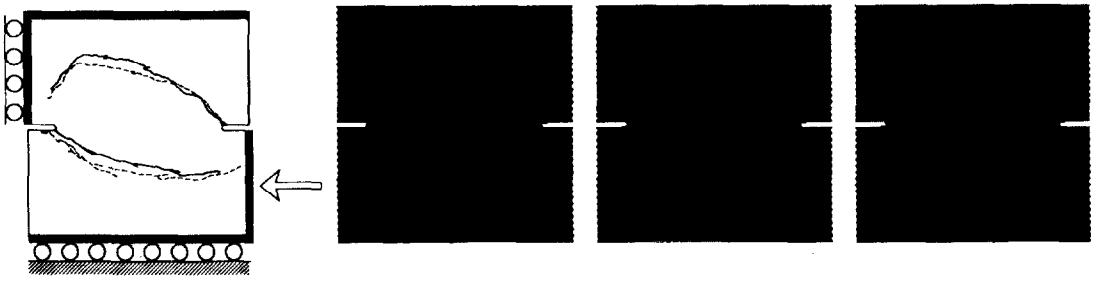

Fig. 2. (a) Geometry and crack pattern of shear experiment on concrete plate, according to ref. [35], simulated crack patterns in mesh with (b) springs, (c) spring and shear elements, and (d) beam elements. (Reprinted from ref. [24].)

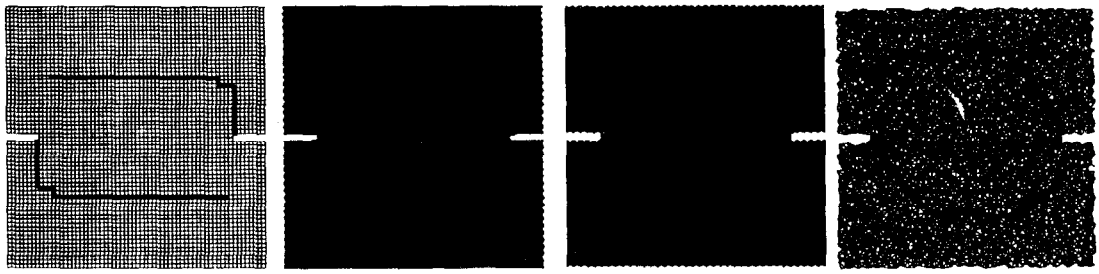

(a) (b) (c) (d)

Fig. 3. Simulated crack patterns in (a) square mesh, (b) regular triangular mesh, (c) rotated triangular mesh and (d) random triangular mesh. (Reprinted from ref.[24].)

ser to the experimentally observed pattern. In all three cases, however, it can also be seen that the crack patterns are influenced by the principal directions of the mesh.

3.2. *Influence of mesh orientation on the crack pattern*

The effect of mesh orientation on crack patterns when using the beam elements with three forces is illustrated in the next example. In Fig. 3, crack patterns are shown of simulations of the same experiment as in the previous section, using four lattices with different beam orientations. In the first mesh, beam elements in a square grid were used [Fig. 3(a)]. The second lattice, shown in Fig. 3(b), is the same as that shown in Fig. 2(d). In the third simulation, shown in Fig. 3(c), a triangular lattice was again used, but the mesh was rotated 90°. In the last simulation [Fig. 3(d)] a special random lattice was used. The cross sections and moments of inertia of the beams in this lattice are chosen in such a way that the lattice represents a homogeneous medium[24], i.e. a uniform applied stress results in a uniform local strain, with no internal relaxations due to the lattice geometry. In all four simulations two overlapping curved cracks were obtained, yet there were differences in crack shape due to the different orientation of the meshes. The simulation using the homogeneous random lattice resembled the experiment most closely. However, for a problem where the randomness of the material is important and is directly implemented in the lattice, it is expected that a regular lattice, as long as the beam size is small with respect to the length scale of the inhomogeneous material, will lead to similar results.

3.3. *Influence of the resolution of the lattice*

We next study the influence of resolution, meaning the number of beams per unit length. The case to be studied is taken from ref.[23]. In this example, we consider that the unit cell of the simulation has a fixed length, and so we are varying the beam length, and thereby the number of beams per unit length of sample. Since we are trying to represent a continuum with a discrete lattice, the resolution of the representation is important. We test the effect of the resolution in this example, where the disorder is implemented at the level of a single beam. A triangular lattice [Fig. 4(b)] having periodic boundary conditions in the horizontal direction is loaded in tension in the vertical direction. The heterogeneity is introduced by randomly assigning two different strengths, in a ratio of 1:3, to the elements, so that the mesh consists of 25% low strength (1.0) and 75% high strength (3.0) elements. Four different analyses were performed, with meshes consisting of 8, 16, 32 and 64 beam elements in the horizontal direction. The length in the horizontal direction is unchanged between simulations.

The crack patterns of the meshes with different element sizes are comparable. However, there is a large difference in load–crack opening response, as seen in Fig. 4(a). The curves are the average response of 10 simulations for each system. The mesh with the lowest resolution (largest beams) shows the most ductile response. This can be explained from the fact that the crack width is larger and thus relatively more energy is released if an element is removed in a coarse mesh compared to a fine mesh, resulting in larger deformations. In any given fracture

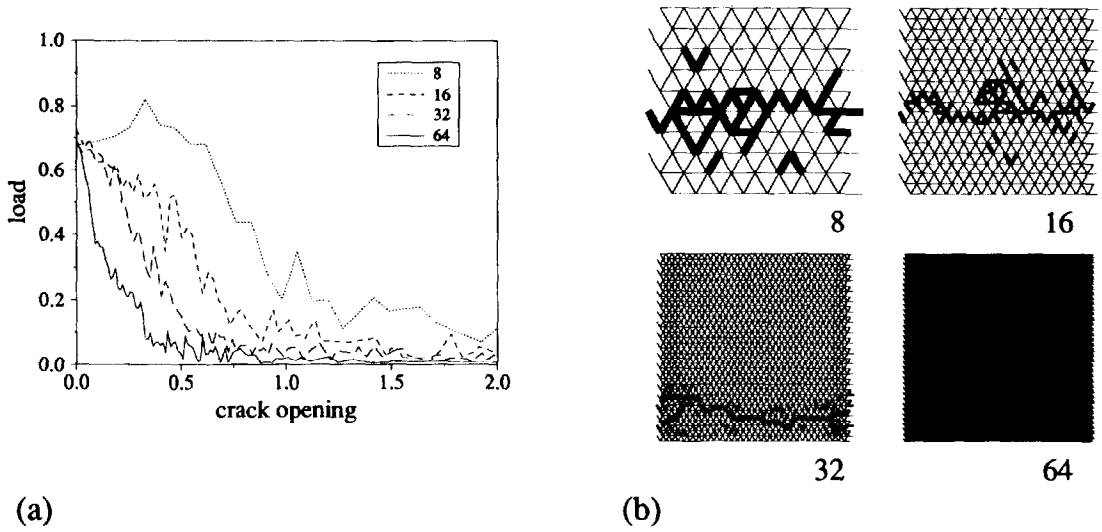

Fig. 4. (a) Load–crack opening and (b) crack patterns for simulations in which the fineness of the mesh was varied. (Reprinted from ref.[23].) Load and crack opening displacement units are arbitrary.

study, the beam resolution should be checked so that one is working in the limit where small changes in the resolution will not have any appreciable effect on the results.

4. FRACTURE LAW

4.1. *Discussion of fracture laws*

In the above simulations the stress in a beam element was calculated using eq. (10), in which the normal force in a beam is divided by the cross section. This procedure does not, however, always give correct results. If a hydrostatic strain is applied to a triangular lattice of beam elements, it is clear that all the elements will carry only normal forces, so that the stresses in all directions are equal. Yet when a uniaxial strain is applied to a uniform triangular lattice, the stress calculated with this fracture law will in general depend on the direction of loading. For example, when a uniaxial strain is applied parallel to one of the principal directions, the beams in this direction will carry more of a load than the beams in the other directions, implying that these 1/3 of the beams will break first in a pattern that reflects the symmetry of the lattice. Other loading directions will produce qualitatively similar results.

In order to illustrate this phenomenon the following analysis was performed. A triangular lattice of beams, with equal properties and having periodic boundary conditions in one direction, was loaded in tension in the other direction, as shown in Fig. 5. When the lattice was loaded in the horizontal (X) direction using the old fracture law, a straight vertical crack was obtained and also a load–crack opening response with a descending branch, as shown in Fig. 5. When the lattice was loaded in the vertical (Y) direction, however, the descending branch stayed high and all the vertical beams in the horizontal "crack" broke first, before all the other beams in the "crack" region. Besides this difference in the crack propagation and the shape of the load–crack opening response, the stress at fracture also depended on the direction of loading. Of course the overall elastic properties are isotropic[31], but the fracture stress depends on how the stress is distributed among the individual bonds. This distribution is different for different directions, hence the directional dependence of the fracture stress. For example, a uniaxial strain in the horizontal direction results in a 33% higher stress at fracture than a uniaxial strain in the vertical direction on the same lattice.

In most of the simulations performed in earlier work[32], the contribution to the stress in the fracture law consisted of the normal force in a beam as well as part of the bending moment. This, however, does not correct the problem of the directionality dependence of the fracture stress in the lattice. Another method would be to combine the normal force and shear force in a beam, as in Mohr's Circles, to obtain a value for the stress in a beam[33,34]. This fracture law

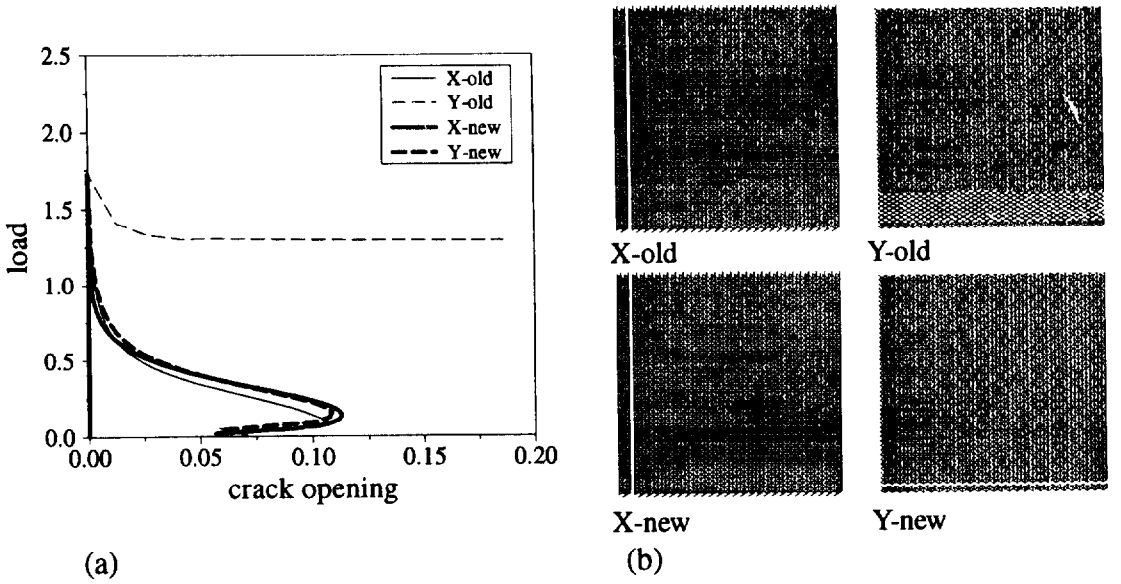

Fig. 5. (a) Load–crack opening and (b) crack patterns for lattice loaded in tension in x- and y-directions using the old and new fracture law. Load and crack opening displacement units are arbitrary.

needs to be checked, but we believe it probably does not correct the directionality problem either.

In the remainder of this section a new fracture law is discussed. The main difference with the aforementioned fracture laws is that the stress is now to be calculated in each node instead of in each beam. All the beams connected to a node contribute to this nodal stress. The procedure for calculating the stress is outlined in Fig. 6. In a node a cut is made, at some angle, like in Fig. 6(a). Out of all the normal and shear forces (the bending moment is not included) in the beams at one side of the cut two resulting forces F_{node} and Q_{node} are computed [Fig. 6(b)]. For the complete range of cut angles between 0 and 2π, the angle is determined for which the normal force is maximal. The shear force for that cut angle is then equal to zero [Fig. 6(c)]. The zero-shear–stress section does not necessarily have to coincide with the symmetry axis, as does the example shown in Fig. 6(c) and (d). The cross sections of the beams in the direction perpendicular to this cut are determined [Fig. 6(d)], a stress σ_{node} is calculated as shown in Fig. 6(e) and is then assigned to each beam attached to this node. Thereafter, the beam that has the maximum value of the ratio of the nodal tensile stress divided by its own tensile strength is broken and removed from the lattice. Note that for a lattice representing a homogeneous material, in which all the beams have an equal strength and stiffness, since all the beams in a node have the same stress they will therefore have the same breaking point. The directionality problem is solved via averaging the stress over the beams attached to one node.

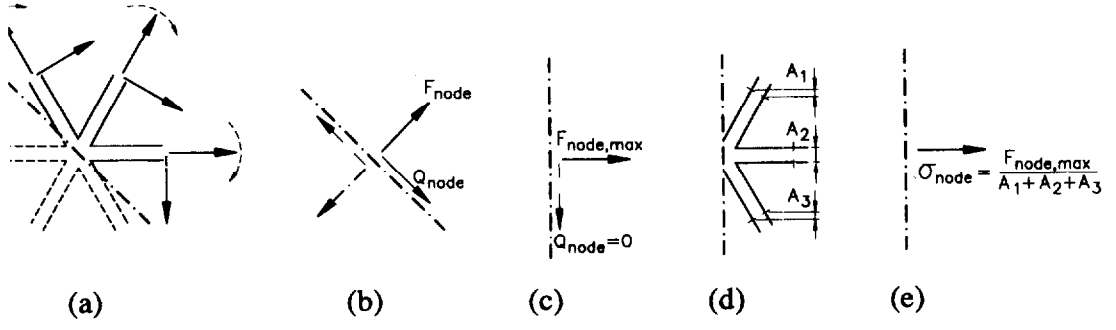

Fig. 6. (a) Lattice with forces in beam elements, (b) resulting normal and shear forces perpendicular to a nodal cut, (c) maximum normal force $F_{\text{node,max}}$, (d) cross sections corresponding to angle with $F_{\text{node,max}}$ and (e) resulting stress in the node.

The relation between the stress found following this procedure, σ_{node}, and the real stress σ (which is the local stress in a medium as a result of a globally applied stress on the lattice) can be determined from the angles in the lattice. The real stress σ is the local stress in a node as a result of a globally applied stress on the lattice. For beam elements with rectangular cross section, unit thickness, and width h, in a triangular lattice, the relation between nodal stress and global stress is:

$$\sigma = \sqrt{3}\frac{h}{l}\sigma_{node}. \tag{11}$$

This new fracture law was applied to the same example as discussed above, the triangular lattice with periodic boundary conditions in one direction and tensile load in the other direction. In Fig. 5 it can be seen that the same crack pattern is now obtained for the lattice loaded in either the X or Y directions. The maximum loads as well as the complete load–crack opening diagrams now match almost perfectly.

4.2. *Compression and splitting in a homogeneous mesh*

In the previous section it was shown that the new fracture law gave good results for uniaxial tensile loading. But what about tensile splitting and compression? In this section simulations with the old and new fracture law are compared for these types of loading. A square section of a triangular lattice of beams having equal properties was used. One beam in the centre was removed to introduce an imperfection for the crack to start. All the loads were applied via nodal displacements. In the case of tensile splitting at each side of the specimen, the two nodes in the middle were displaced in the loading direction. Perpendicular to the loading direction the displacement of these two nodes were fixed. In the case of compression, all the nodes at the edge were given an equal displacement in the loading direction. Perpendicular to the loading direction the nodes were free to move.

The resulting crack patterns are plotted in Fig. 7 (the displacements shown in Figs 7 and 9 have been exaggerated in order to visualize the responses adequately—the model does not actually take large displacements into account). Figure 7(a) and (b) shows the crack patterns for a lattice loaded in tensile splitting in the horizontal and vertical directions, respectively, using the old fracture law. In the simulations shown in Fig. 7(e) and (f) the new fracture law was used for

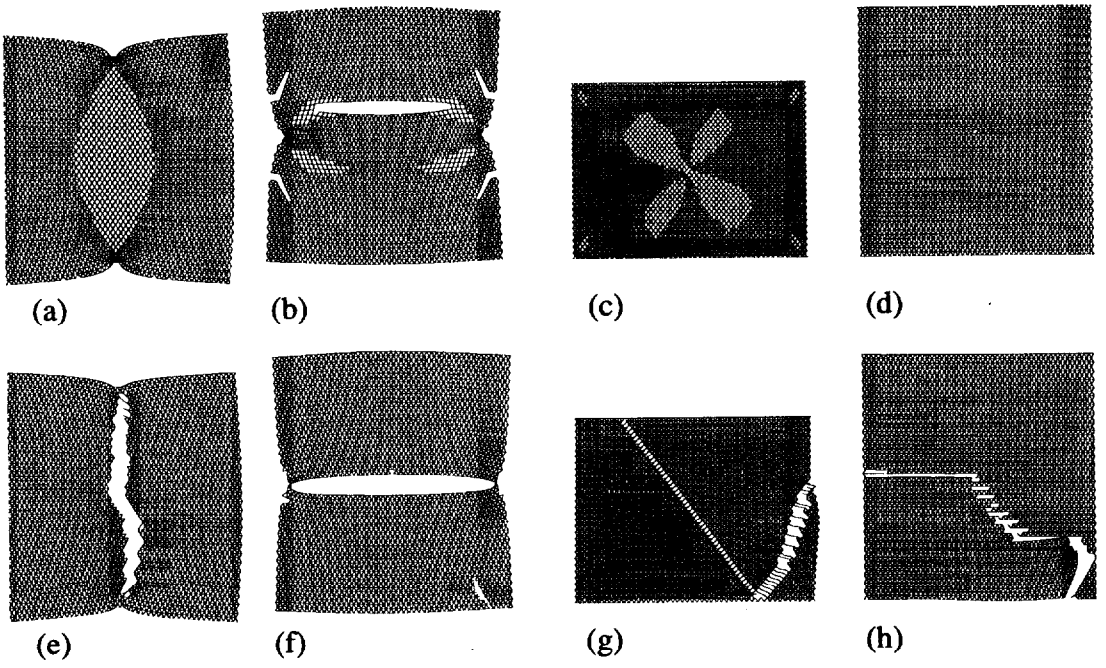

Fig. 7. Crack patterns for a lattice loaded in tension splitting (S) or compression (C) in either the vertical (V) or horizontal (H) directions using the old (O) or new (N) fracture laws: (a) S–V–O, (b) S–H–O, (c) C–V–O, (d) C–H–O, (e) S–V–N, (f) S–H–N, (g) C–V–N, and (h) C–H–N.

the same loading case. When using the old fracture law with tensile splitting in the vertical direction [Fig. 7(a)], the same phenomenon is observed as in the tensile simulation of the previous section (Fig. 5). Only the beams in the direction of the tensile stress fail, thus showing up as a lighter region because 1/3 of the beams are missing. In the simulation of Fig. 7(b) some splitting behaviour is found, yet the crack is not in the middle where it should be. With the new fracture law the simulated crack patterns show a much improved behaviour, and, although not shown here, the load–crack opening response for both loading directions do match when using the new fracture law.

In Fig. 7(c) and (d) [old fracture law] and Fig. 7(g) and (h) [new fracture law] the crack patterns are shown for a lattice loaded in compression in either the horizontal or vertical directions. There was no assumed constraint at the supports. With the old fracture law rather strange crack patterns are observed [Fig. 7(c)], and the lattice loaded in the horizontal direction [Fig. 7(d)] did not fracture at all, since the normal forces in all the beams were compressive. The simulations with the new fracture law [Fig. 7(g) and (h)] again show improved behaviour. However, it should be mentioned that the crack patterns for compression, also with the new fracture law, are still somewhat influenced by the preferred directions in the triangular mesh. As discussed in Section 3.2, a random lattice would give better results. However, a regular lattice with implemented heterogeneity can also remove this directional dependency, as will be shown in the next section.

4.3. *Simulation vs experiment: concrete fracture*

In the previous sections some numerical features of the lattice modelling of fracture were illustrated. All cases were studied with a homogeneous lattice. Yet the actual goal of the lattice approach is to simulate fracture in a real material. Real materials are in general random and inhomogeneous, and therefore fracture will be influenced by the microstructure of the material. Heterogeneity has to be implemented to simulate the fracture process correctly. The scale at which information is required should be taken into account too. Different techniques have been used in the past to implement disorder. These techniques all have their own application (scale) for which they will give good results. Different options include:

- Randomly assigning different properties, possibly following some kind of a distribution, to the elements in the lattice[32,28].
- Using a mesh with random geometry, but equal properties for the beams[32,27].
- Generating a microstructure and projecting on this a regular lattice of beams, assigning different properties to the beams depending on their position[3,5].
- Using a combination of a random geometry and a generated grain structure[2].

In the simulations shown in this section a different method was used in which the microstructure was implemented in a direct way from an image of a real piece of material, such as in the left image of Fig. 8, which is a scanning electron micrograph of a mortar specimen. By using image processing techniques the image is split into three phases: sand grains, cement paste matrix and voids (middle image in Fig. 8). A lattice of beam elements is projected on top of this image and different properties are assigned to the elements in the different zones (right image in

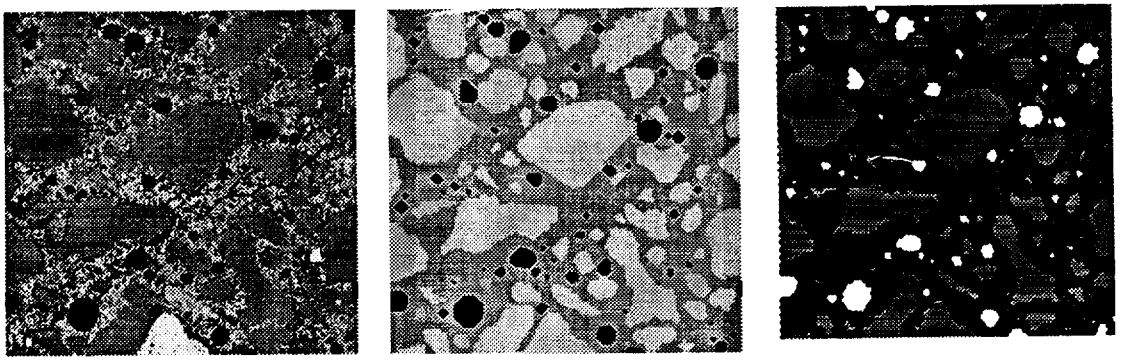

Fig. 8. Left: digital image of SEM micrograph of a mortar, middle: three-phase image after processing and right: lattice of beams showing different properties for the elements.

Fig. 8). The elements in the sand, the cement paste matrix and the interface between were given strengths and stiffnesses in the ratios: 10, 4 and 2, respectively [32]. No elements were placed in the voids. The purpose of the simulations was not to find a quantitative match with the load vs crack opening experimental curves, but to show that the qualitative trends were similar to what happens in the real material.

Four simulations were performed using the mesh shown in Fig. 8 (right image). The loading cases were uniaxial tension [Fig. 9(a)], tensile splitting [Fig. 9(b)] and two compression cases [Fig. 9(c) and (d)]. The new fracture law that was introduced in Section 4.1 was used. In the uniaxial tension simulation (load in the vertical direction), shown in Fig. 9(a), cracks started from both sides of the specimen, because no rotation of the ends was allowed. Pieces of material still bridging the two crack faces can be seen, as has been observed experimentally [39]. This causes a ductile response. In the tensile splitting case (vertical direction point loads) [Fig. 9(b)] a crack started in the centre of the specimen and propagated to the loading points. The stress–crack opening curves for the two tension cases are plotted in Fig. 12(a). Both show a softening behaviour. The stress in the splitting case is about 16% higher than the stress in the uniaxial tension case, which is comparable to what is observed experimentally.

For the compression case the boundary conditions were varied. In the simulation shown in Fig. 9(c) the nodes where the vertical compressive loads were applied were free to move horizontally (zero boundary restraint). In the other case [Fig. 9(d)] these nodes were fixed (infinite boundary restraint). In the case of free boundaries [Fig. 9(c)] diagonal cracks, or shear bands, are found. Fixed boundaries [Fig. 9(d)] lead to hourglass type crack patterns. This behaviour has also been observed experimentally [40]. The computing time needed for the simulations depends on the size of the mesh, the degree of heterogeneity and the amount of elements needed to crack. On a Silicon Graphics R4600 workstation, the analysis required for Fig. 9(a) ran for

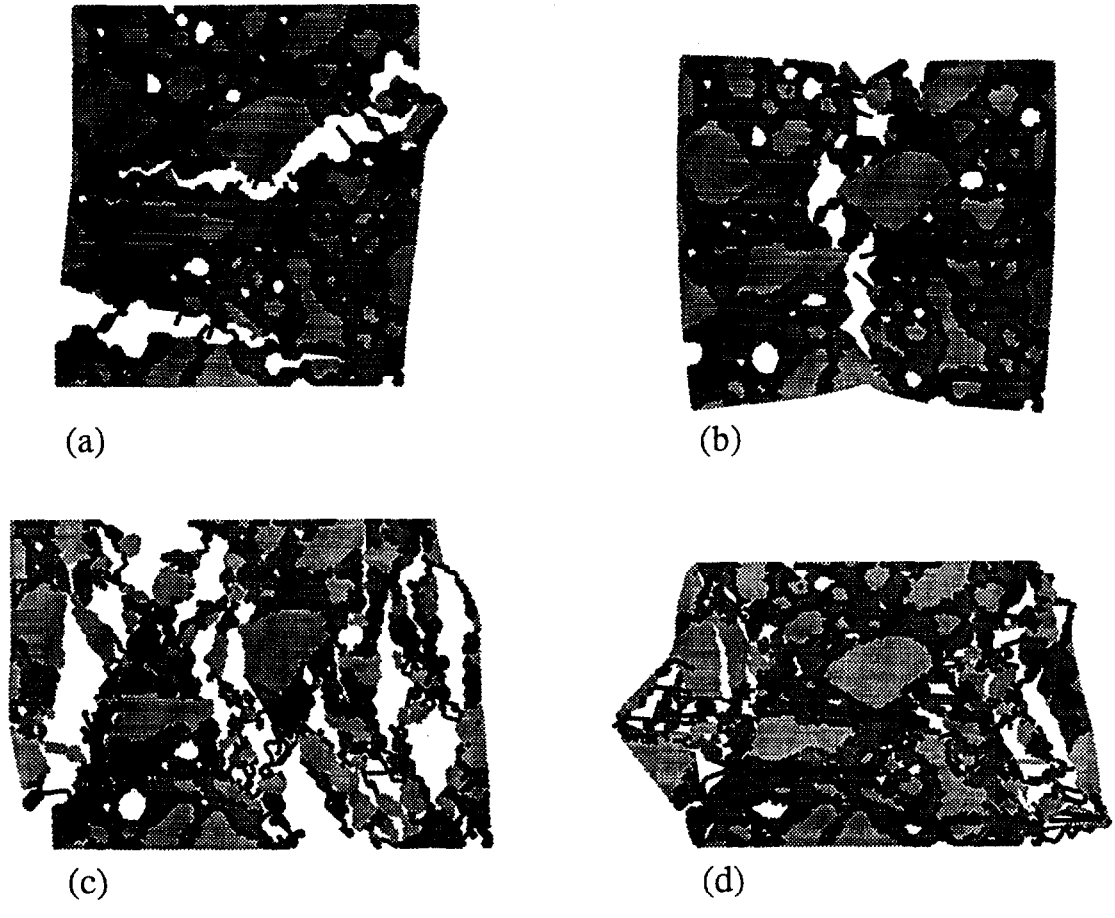

Fig. 9. Crack patterns for the lattice of Fig. 8 loaded in: (a) tension, (b) tensile splitting, (c) compression (free boundaries) and (d) compression (fixed boundaries).

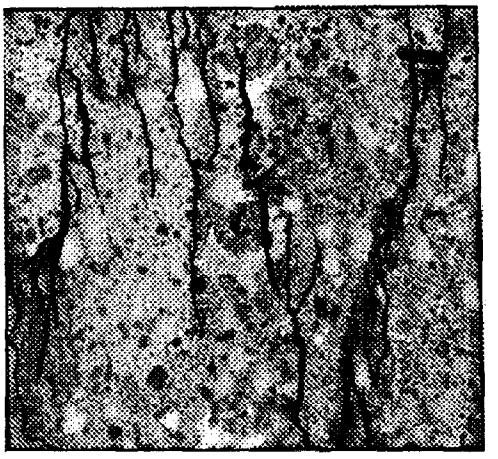

Fig. 10. Experimentally observed crack pattern for specimen loaded in compression between supports with low friction (reprinted with permission from ref.[40]).

about eight hours. About 400 beam elements had to be removed from the mesh in order to crack the specimen. The analysis required for Fig. 9(c) took about 10 times longer, because the amount of elements that had to be fractured was 10 times larger.

Experimental[40] crack patterns found in laboratory specimens on concrete cubes vertically loaded in compression are shown in Figs 10 and 11 (reprinted with permission from ref. [40]). Figure 10 shows a specimen tested between low friction supports. The specimen in Fig. 11 was tested between supports with high friction. Similarities between simulation and experiment can be seen.

The stress–crack opening diagrams for the compression simulations of Fig. 9(c) and (d) are plotted in Fig. 12(b). Compared with the real behaviour of concrete the simulated results are only in qualitative agreement. For the simulation with free boundaries a softening behaviour was obtained. For the fixed case no descending branch was found. Of course this is different from what is found experimentally. However, there are two major differences between the simulation shown and an experiment with fixed boundaries. First, in an experiment the boundaries are never completely fixed (restrained). Second, the three-dimensional effect due to the boundary restraint becomes very important. A two-dimensional simulation is not sufficient in that case. Finally, in the beam lattice two free pieces of material can pass right through each other, in contrast to a real material, where frictional forces can be important. A comparison of the maximum stress in the uniaxial tensile case with the compression case with free boundaries shows that the stress in the compression case is about 10 times higher, a realistic ratio for concrete.

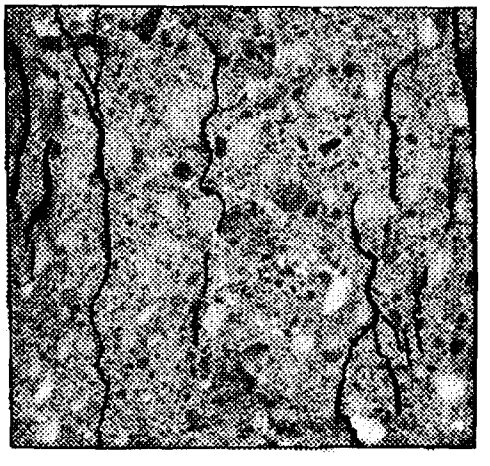

Fig. 11. Experimentally observed crack pattern for specimen loaded in compression between supports with high friction (reprinted with permission from ref.[40]).

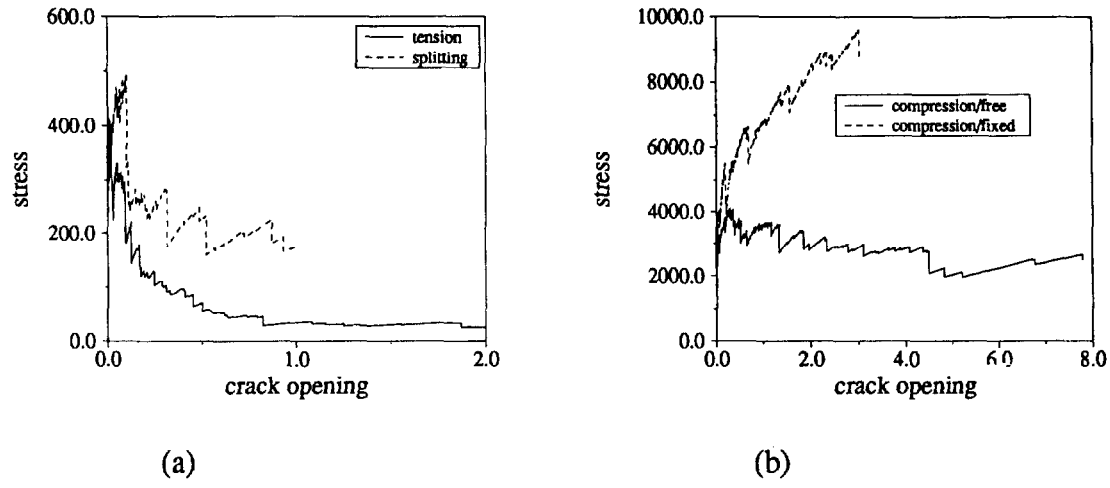

Fig. 12. Stress–crack opening diagrams for crack patterns shown in Fig. 9: (a) tension and tensile splitting, and (b) compression with free and fixed boundaries. Load and crack opening displacement units are arbitrary.

5. DISCUSSION AND CONCLUSIONS

In this paper numerical aspects of lattice models for the simulation of fracture were discussed, with the emphasis being on crack patterns obtained as a function of the kinds of loading and boundary conditions used. It was shown that lattice models should be used with care. Sometimes results that are found are caused by the model and not by the behaviour of the material that is being modelled.

The element type used strongly influenced the simulated crack patterns obtained. Beam elements with three degrees of freedom per node seem to give the best agreement with experimentally obtained crack patterns. The orientation of the beams in the lattice also influenced the simulated crack patterns, with the cracks tending to follow the mesh lines. This disadvantage can be circumvented by using a random lattice that is made elastically homogeneous. The simulation results obtained also depended on the resolution of the lattice. The stress–strain behaviour became more ductile for decreasing resolution of the elements.

A new fracture law has been proposed that uses the maximum tensile stress in each node to determine which beam element should be fractured. In contrast to fracture laws used previously, the fracture stress that is determined in this manner does not depend on the direction of the applied loading.

In Section 5 a method was outlined to implement the heterogeneity of a material in a direct way. A digital image of the microstructure of a mortar was used to assign different properties to the elements in the lattice. A lattice in which heterogeneity was implemented following this method was subjected to a few basic loading conditions. Realistic crack patterns were obtained from these simulations. However, the problem that still remains is how to determine the input parameters for strength and stiffness for the elements in the lattice. For concrete, data for the strength and stiffness of the interfacial zone between aggregates and cement paste matrix are unknown. A combined experimental and numerical investigation[41] should lead to appropriate values.

Finally, the use of lattice models to analyse structural members on a material level is at present not realistic. The amount of computer memory and computing power necessary to store and analyse a beam lattice large enough to simulate the material aspects of a structure of the order of a meter in size are at present prohibitive. The use of lattice models, however, can be very helpful in studying the fracture behaviour of a material and how this behaviour will change if the properties of the individual components change. Lattice models can be a useful tool for developing stronger and better materials if they are made part of the material design process.

Acknowledgements—This work has been made possible by a fellowship of the Royal Netherlands Academy of Arts and Sciences (KNAW). Fruitful discussions with J. G. M. van Mier, A. Vervuurt and M. R. A. van Vliet are acknowledged.

The hospitality of NIST, Gaithersburg, Maryland, U.S.A. and Stevin Laboratory, at the Delft University of Technology, Delft, The Netherlands, where part of this research took place, are both gratefully appreciated. The authors thank P. A. Stutzman of NIST for obtaining and processing the scanning electron micrograph shown in Fig. 8. The authors gratefully acknowledge the permission of M. R. A. van Vliet and J. G. M. van Mier to reprint Figs 10 and 11.

REFERENCES

1. Herrmann, H. J. and Roux, S., *Statistical Models for the Fracture of Disordered Media*. North-Holland, Amsterdam, 1990.
2. Bažant, Z. P., Tabbara, M. R., Kazemi, M. T. and Pijaudier-Cabot, G., Random particle model for fracture of aggregate or fibre composites. *J. Engng Mech. ASCE*, 1990, **116**, 1686–1705.
3. Schlangen, E. and van Mier, J. G. M., Experimental and numerical analysis of micromechanisms of fracture of cement-based composites. *Cem. Concr. Comp.*, 1992, **14**, 105–118.
4. Curtin, W. A. and Scher, H., Brittle fracture in disordered materials: a spring network model. *J. Mater. Res.*, 1990, **5**, 535–553.
5. Jagota, A. and Bennison, S. J., Spring-network and finite-element models for elasticity and fracture. In *Breakdown and Non-Linearity in Soft Condensed Matter*, ed. K. K. Bardhan *et al.* Springer Verlag, Berlin, 1994.
6. Delaplace, A., Pijaudier-Cabot, G. and Roux, S., Progressive damage in discrete models and consequences on continuum modelling. *J. Mech. Phys. Solids*, 1996, **44**, 99–136.
7. Ostoja-Starzewski, M., Sheng, P. Y. and Jasiuk, I., Influence of random geometry on effective properties and damage formation in 2-D composites. *ASME J. Engng Mater. Tech.*, 1994, **116**, 384–391.
8. Jagota, A. and Bennison, S. J., Element breaking rules in computational models for brittle materials. *Modelling Simul. Mater. Sci. Engng*, 1995, **3**, 485–501.
9. Ostoja-Starzewski, M. and Lee, J.-D., Damage maps of disordered composites: a spring network approach. *Int. J. Fracture*, 1996, **75**, R51–557.
10. Phoenix, S. L., Approximations for the strength distribution and size effect in an idealized lattice model of material breakdown. *J. Mech. Phys. Solids*, 1991, **39**, 173–200.
11. Duxbury, P. M., Beale, P. D. and Moukarzel, C., Breakdown of two-phase random resistor networks. *Phys. Rev. B*, 1995, **51**, 3476–3482.
12. Grah, M., Alzebdeh, K., Sheng, P. Y., Vaudin, M. D., Bowman, K. J. and Ostoja-Starzewski, M., Brittle intergranular failure in 2-D microstructures: experiments and computer simulations. *Acta Mater.*, in press, 1996.
13. Duxbury, P. M., Breakdown of diluted and hierarchical systems. In *Statistical Models for the Fracture of Disordered Media*, ed. H. J. Herrmann and S. Roux. Elsevier Science Publishers, Amsterdam, 1990, pp. 189–228.
14. Paskin, A., Gohar, A. and Dienes, G. J., Computer simulation of crack propagation. *Phys. Rev. Lett.*, 1980, **44**, 940–943.
15. Ray, P. and Chakrabarti, B. K., The critical behavior of fracture properties of dilute brittle solids near the percolation threshold. *J. Phys. C: Solid State Phys.*, 1985, **18**, L185–L188.
16. Ray, P. and Chakrabarti, B. K., A microscopic approach to the statistical fracture analysis of disordered brittle solids. *Solid State Communications*, 1985, **53**, 477–479.
17. Meakin, P., A simple model for elastic fracture in thin films. *Thin Solid Films*, 1987, **151**, 165–190.
18. Skjeltorp, A. T. and Meakin, P., Fracture in microsphere monolayers studied by experiment and computer simulation. *Nature*, 1988, **335**, 424–426.
19. Beale, P. D. and Srolovitz, D. J., Elastic fracture in random materials. *Phys. Rev. B*, 1988, **37**, 5500–5507.
20. Srolovitz, D. J. and Beale, P. D., Computer simulation of failure in an elastic model with randomly distributed defects. *J. Am. Ceram. Soc.*, 1988, **71**, 362–369.
21. Harlow, D. G. and Phoenix, S. L., Approximations for the strength distribution and size effect in an idealized lattice model of material breakdown. *J. Mech. Phys. Solids*, 1991, **39**, 173–200.
22. Bentz, D. P., Schlangen, E. and Garboczi, E. J., Computer simulation of interfacial zone microstructure and its effect on the properties of cement-based composites. In *Materials Science of Concrete IV*, ed. J. Skalny and S. Mindess. American Ceramic Society, Westerville, Ohio, 1995.
23. Schlangen, E., Fracture simulations of brittle heterogeneous materials. In *Proc. 10th ASCE-EMD Conference*, ASCE, 1995, pp. 130–133.
24. Schlangen, E. and Garboczi, E. J., New method for simulating fracture using an elastically uniform random geometry lattice. *Int. J. Engng Sci.*, 1996, **34**, 1131–1144.
25. Cook, R. D., Malkus, D. S. and Plesha, M. E., *Concepts and Applications of Finite Element Analysis*. J. Wiley, New York, 1989.
26. Press, W. H., Teukolsky, S. A., Vettering, W. T. and Flannery, B. P., *Numerical Recipes in C*. Cambridge University Press, Cambridge, 1988.
27. Garboczi, E. J. and Day, A. R., An algorithm for computing the effective linear elastic properties of heterogeneous materials: 3-D results for composites with equal phase Poisson ratios. *J. Mech. Phys. Solids*, 1995, **43**, 1349–1362.
28. Batrouni, G. G. and Hansen, A., Fourier acceleration of iterative processes in disordered systems. *J. Stat. Phys.*, 1988, **52**(3/4), 747–773.
29. Majid, K. I., Saka, M. P. and Celik, T., The theorems of structural variation generalized for rigidly jointed frames. *Proc. Inst. Civ. Engrs, Part* 2, Vol. 65, 1978, pp. 839–856.
30. Jirásek, M. and Bažant, Z. P., Macroscopic fracture characteristics of random particle systems. *Int. J. Fracture*, 1995, **69**, 201–228.
31. Feng, S., Thorpe, M. F. and Garboczi, E. J., Effective-medium theory of percolation on central-force elastic networks. *Phys. Rev. B*, 1985, **31**, 276–280.
32. Schlangen, E., Experimental and numerical analysis of fracture processes in concrete. Ph.D. Thesis, Delft University of Tech., The Netherlands, 1993.
33. Beranek, W. J. and Hobbelman, G. J., Constitutive modelling of structural concrete as an assemblage of spheres. In *Computer Modelling of Concrete Structures*, ed. H. Mang *et al.* Pineridge Press, Swansea, 1994, pp. 37–51.

34. van Vliet, M. R. A. and van Mier, J. G. M., Comparison of lattice type fracture models for concrete under biaxial loading regimes. In *Size-Scale Effects in the Failure Mechanisms of Materials and Structures*, ed. A. Carpinteri. E&FN Spon, London, 1994.
35. Nooru-Mohamed, M. B., *Mixed Mode Fracture of Concrete: an Experimental Approach.* Ph.D. Thesis, Delft University of Tech., The Netherlands, 1992.
36. Meakin, P., Li, G., Sander, L. M., Louis, E. and Guinea, F., A simple two-dimensional model for crack propagation. *J. Phys. A: Math. Gen.*, 1989, **22,** 1393–1403.
37. Burt, N. J. and Dougill, J. W., Progressive failure in a model heterogeneous medium. *J. Engng Mech. Div. ASCE*, 1977, **103,** 365–376.
38. Herrmann, H. J., Hansen, H. and Roux, S., Fracture of disordered, elastic lattices in two dimensions. *Phys. Rev. B*, 1989, **39,** 637–648.
39. van Mier, J. G. M., Mode I fracture of concrete: discontinuous crack growth and crack interface grain bridging. *Cem. and Concr. Res.*, 1991, **21,** 1–15.
40. van Vliet, M. R. A. and van Mier, J. G. M., Softening behaviour of concrete under uniaxial compression. In *Fracture Mechanics of Concrete Structures*, ed. F. H. Wittmann. AEDIFICATIO, Freiburg, 1995, pp. 383–396.
41. Vervuurt, A. and van Mier, J. G. M., Interface fracture in cement-based materials. In *Fracture Mechanics of Concrete Structures*, ed. F. H. Wittmann. AEDIFICATIO, Freiburg, 1995, pp. 295–304.

(*Received* 22 *January* 1996)